

# The principle of gating charge movement in a voltage-dependent K<sup>+</sup> channel

Youxing Jiang\*, Vanessa Ruta, Jiayun Chen, Alice Lee & Roderick MacKinnon

Howard Hughes Medical Institute, Laboratory of Molecular Neurobiology and Biophysics, Rockefeller University, 1230 York Avenue, New York, New York 10021, USA

**The steep dependence of channel opening on membrane voltage allows voltage-dependent K<sup>+</sup> channels to turn on almost like a switch. Opening is driven by the movement of gating charges that originate from arginine residues on helical S4 segments of the protein. Each S4 segment forms half of a 'voltage-sensor paddle' on the channel's outer perimeter. Here we show that the voltage-sensor paddles are positioned inside the membrane, near the intracellular surface, when the channel is closed, and that the paddles move a large distance across the membrane from inside to outside when the channel opens. KvAP channels were reconstituted into planar lipid membranes and studied using monoclonal Fab fragments, a voltage-sensor toxin, and avidin binding to tethered biotin. Our findings lead us to conclude that the voltage-sensor paddles operate somewhat like hydrophobic cations attached to levers, enabling the membrane electric field to open and close the pore.**

Voltage-dependent K<sup>+</sup> channel opening follows a very steep function of membrane voltage<sup>1</sup>. To allow channels to switch to the open state, gating charges—charged amino acids on the channel protein—move within the membrane electric field to open the pore<sup>1–3</sup>. The crystal structure of KvAP, a voltage-dependent K<sup>+</sup> channel, suggests how these gating charge movements might occur<sup>4</sup>. Four arginine residues are located on a predominantly hydrophobic helix–turn–helix structure called the voltage-sensor paddle. One paddle on each subunit is present at the outer perimeter of the channel. By moving across the membrane near the protein–lipid interface, the paddles could carry the arginine residues through the electric field, coupling pore opening to membrane voltage. We test this hypothesis for the movement of gating charges by estimating the positions of the voltage-sensor paddles inside the membrane when the channel is closed and opened.

## Using Fabs and a toxin to detect paddle motions

Two monoclonal Fabs, 6E1 and 33H1, were used to crystallize and determine the structures of the full-length KvAP channel and the isolated voltage sensor, respectively<sup>4</sup>. Both Fabs were found attached to the same epitope on the tip of the voltage-sensor paddle between S3b and S4. We used these same Fabs to examine the position of the voltage-sensor paddles when the KvAP channel functions in lipid membranes (Fig. 1a), and to assess whether they change their position when the channel gates open in response to membrane depolarization. Figure 1b shows that both the 6E1 and 33H1 Fabs inhibit channel function when applied to the external solution. By contrast, neither Fab affected channel function from the internal solution.

Inhibition by external Fabs requires membrane depolarization (Fig. 1c). When the 33H1 Fab is added to the external chamber while the channel is held closed at  $-100$  mV for 10 min (Fig. 1c, interval between the black and red data points), no inhibition is observed. The slightly larger current of the first red data point (20-min point) reflects recovery from a small amount of steady-state inactivation of channels occurring during the control pulse period (0–10-min data points)<sup>5</sup>. The important point, however, is that inhibition of current is detectable only on the second pulse following the addition of the Fab, as if the channel has first to open in order for the Fabs to bind. Inhibition progresses as the membrane is repeatedly depolarized. We also observe gradual recovery from

inhibition if, once the Fabs are bound, the membrane is held at a negative voltage for a prolonged period (30–40-min interval), implying that negative membrane voltages destabilize the interactions between channels and Fabs, causing the Fabs to dissociate. The same properties of inhibition are observed for Fab 6E1. Based on these results, we conclude that the voltage-sensor paddles must remain inaccessible as long as the channel is held closed by the negative membrane voltage, and that the entire epitope (two helical turns of S3b and one turn of S4) becomes exposed to the external side in response to depolarization.

Why do the Fabs inhibit the channel? If they bind to the voltage-sensor paddles from the external side when the membrane is depolarized, why do the Fabs not simply hold the channel permanently open? Inhibition can be explained by the fact that the KvAP channel, like most voltage-dependent K<sup>+</sup> channels, inactivates<sup>5</sup>. That is, its pore stops conducting ions spontaneously during prolonged depolarizations of the membrane, even though the voltage sensors remain in their open conformation. Inactivation could also occur when the Fabs bind and hold the voltage sensors in their open conformation, thus explaining inhibition.

It is interesting that tarantula venom toxins also bind to residues on S3 and S4 (ref. 6), which we now know to be on the voltage-sensor paddles<sup>4</sup>. On addition of an approximately half-inhibitory concentration of the tarantula venom toxin VSTX1 to the external side of KvAP, we observe that the rate of inhibition is faster if the membrane is depolarized at a higher frequency (Fig. 1d). Therefore, the toxins, like the Fabs, require membrane depolarization.

We conclude from experiments with Fab fragments and a tarantula venom toxin that the voltage-sensor paddles are exposed to the extracellular solution during membrane depolarization (positive inside) but not during hyperpolarization (negative inside). In view of the KvAP crystal structure<sup>4</sup>, these results imply that the voltage-sensor paddles can move a large distance across the lipid membrane. How deep inside the membrane do the paddles sit when the membrane is hyperpolarized, and how far do they move when the channel opens?

## Using biotin and avidin to measure paddle motions

Finkelstein and co-workers used avidin binding to biotinylated colicin to examine the movements of its components across the lipid bilayer<sup>7–9</sup>. We subjected the KvAP channel to a similar analysis. The idea behind the experiments is outlined in Fig. 2a. We introduce cysteine residues at specific locations in the channel, biotinylate the cysteine, reconstitute channels into planar lipid membranes, and

\* Present address: University of Texas Southwestern Medical Center, Department of Physiology, 5323 Harry Hines Blvd, Dallas, Texas 75390-9040, USA.

then determine whether avidin binds from the internal or external side, and whether binding depends on membrane depolarization. Wild-type KvAP channels contain a single cysteine on the carboxy-terminus, which was mutated to serine (without affecting function) to work with a channel without background cysteine residues.

The crystal structure of avidin and the chemical structure of biotin attached to its linker are shown in Fig. 2b. Biotin binds within a deep cleft inside the core of avidin, a rigid protein molecule<sup>10</sup>. The atom on the biotin molecule to which the linker is attached is 7 Å beneath the surface of avidin (Fig. 2b). Therefore, when avidin binds to a biotinylated cysteine on the channel, the distance from the cysteine α-carbon to the surface of avidin is 10 Å; this is the pertinent linker length from the α-carbon to avidin. Since avidin is large (the tetramer is a 57-kDa protein), it cannot fit into clefts on the channel and therefore cannot penetrate the surface. The important point is that, for avidin to bind to a tethered biotin, the cysteine α-carbon has to be within 10 Å of the bulk aqueous solution on either side of the membrane. Applying this restraint, we used linked biotin and avidin as a molecular ruler to measure positions of the voltage-sensor paddles.

Detection of avidin binding to biotinylated channels depends on the demonstration of a functional effect when avidin ‘grabs’ tethered biotin. Control experiments and examples are illustrated in Fig. 2c. Our convention for representing data will be black, red and blue traces corresponding to control (no avidin), external and internal avidin, respectively. Biotinylated wild-type channels are not affected by external avidin and show a small reduction in current when avidin is applied to the internal solution. On the basis of

protein gel assays, we conclude that the wild-type channels do not contain detectable biotin on them after the biotinylation procedure (not shown). Three examples of biotinylated cysteine mutant channels are shown. The G112C mutant is inhibited completely by external but not internal avidin; the small reduction by internal avidin is similar to the wild-type control. The I127C mutant is inhibited completely by internal but not by external avidin. The L103C mutant shows an outcome different from complete inhibition: external avidin reduces the current but does not abolish it, and changes the kinetics of current activation. Another outcome that is observed at certain positions is partial inhibition by avidin without changing the gating kinetics (Fig. 3). These cases probably reflect incomplete biotinylation of buried cysteine residues. We excluded the possibility that ‘no effect’ (that is, internal avidin on G112C or external avidin on I127C) represents ‘silent’ avidin binding by adding avidin first to the ‘no effect’ side of the membrane and then to the opposite side (not shown). Because avidin binding to biotin is essentially irreversible, silent binding to one side should protect from binding to the other, but this was never observed. Thus, ‘no effect’ signifies no binding.

Data from a scan of the voltage-sensor paddles from amino-acid position 101 on S3b to position 127 on S4 are shown in Fig. 3. Positions were mutated individually to cysteine, biotinylated and studied in planar lipid membranes. Certain biotinylated mutants showed altered gating even before avidin addition (for example, valine 119), or appeared to be less abundant in the membrane (for example, leucine 121). But in all cases, channels could be held closed at negative membrane voltages (typically –100 mV) and opened by

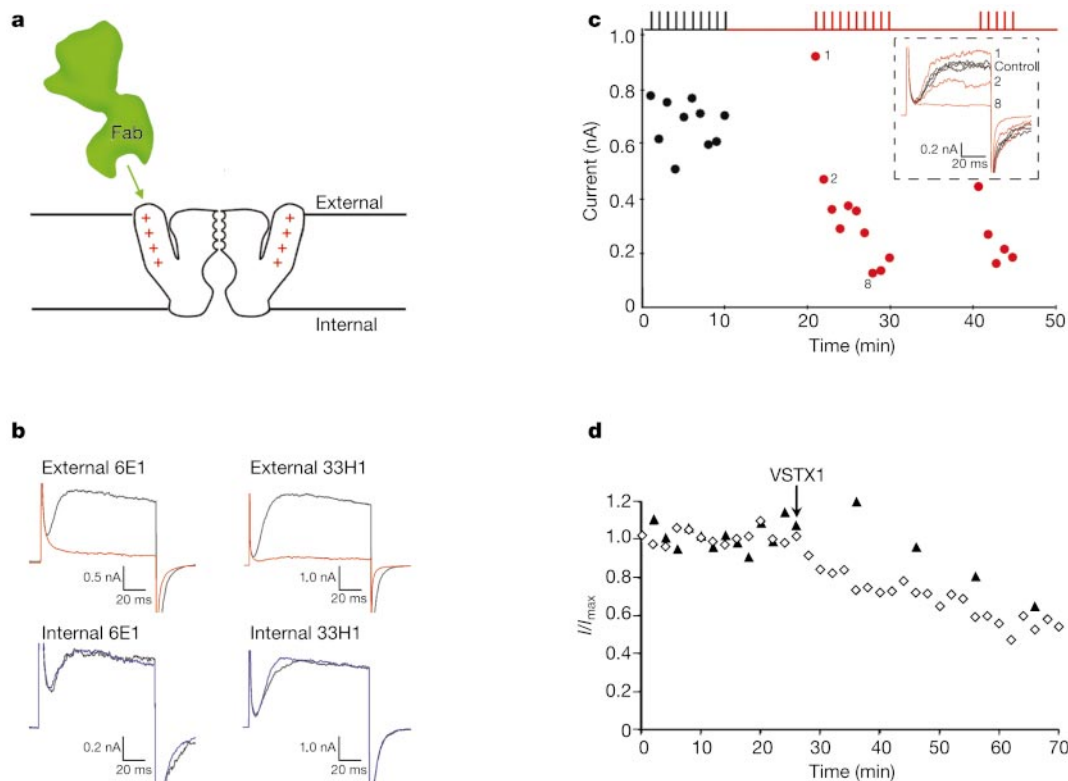


**Figure 1** Inhibition of KvAP channels by Fabs and a tarantula venom toxin that bind to the voltage-sensor paddles. **a**, Experimental strategy: Fab (green) is added to the external or internal side of a planar lipid membrane to determine whether the epitope is exposed. **b**, Fabs used in crystallization (6E1 and 33H1) inhibit from the external (red traces) but not the internal (blue traces) side of the membrane. Currents before (black traces) and after the addition of about 500 nM Fab (red and blue traces) were elicited by membrane depolarization to 100 mV from a holding voltage of –100 mV. **c**, Fab 33H1 binds to the voltage-sensor paddle only when the membrane is depolarized. Current elicited by

depolarization from –100 mV to 100 mV at times indicated by the stimulus trace (above) in the absence (black symbols) or presence of 500 nM Fab (red symbols) is presented as a function of time. Selected current traces corresponding to the numbered symbols are shown (inset). **d**, VSTX1 binds from the external side only when the membrane is depolarized. Currents, normalized to the average control value, were elicited by a 100-ms depolarization to 100 mV every 120 s (diamonds) or every 600 s (triangles). VSTX1 (30 nM) was added to the external solution at the point indicated by the arrow.

membrane depolarizations (typically 100 mV for 200 ms) every 120 s. To compensate for mutations that shifted the voltage-activation curve, we sometimes held the membrane as negative as  $-140$  mV, or used opening depolarizations as positive as 200 mV. Avidin bound to the tethered biotin and affected channel function at all positions studied. In many cases, avidin caused complete inhibition, and in some cases partial inhibition with altered kinetics. Partial inhibition at certain sites (for example, leucine 110 and leucine 122) can be explained on the basis of incomplete biotinylation because the side chain is buried within the 'core' of the voltage-sensor paddle between S3b and S4. This finding is consistent with the proposal that S3b and S4 move together as a voltage-sensor paddle unit.

We are most interested in whether a particular position on the voltage-sensor paddle allows binding to avidin from the external or internal solution. Amino acids on the paddle are colour-coded according to the membrane side from which avidin bound: red, outside; blue, inside; yellow, both. For avidin binding from the external side, we examined whether membrane depolarization is required, by studying the effect of depolarization frequency on the rate of channel inhibition by avidin (Fig. 4). Inhibition from the external solution required depolarization: higher frequencies gave

higher rates of inhibition. In other words, the voltage-sensor paddles can be protected from external avidin binding by keeping the membrane at negative voltages, and the paddles are exposed to external avidin at positive voltages. This was the case for all external positions (Fig. 3, red and yellow).

However, protection from inhibition by external avidin, Fabs and a voltage-sensor toxin, by holding the membrane at negative voltages, is incomplete. In particular, if the wait at negative voltages is long enough, inhibition occurs but at a low rate (Fig. 4). This finding is explained on the basis of thermal fluctuations of the voltage sensors. Probably four voltage-sensor paddles have to move to open the pore<sup>1,11–13</sup>. But individual paddle movements must occasionally occur even at negative voltages. These sensor movements underlying incomplete protection are consistent with gating currents preceding pore opening<sup>2</sup>, and longer delays before pore opening when the membrane is depolarized from more negative holding voltages, a phenomenon known as the Cole–Moore effect<sup>14</sup>.

Biotin molecules tethered at two positions were captured by avidin from both sides of the membrane (121 and 122; Fig. 3, yellow). At these positions, inhibition was complete from either side alone, because subsequent addition of avidin to the opposite side caused no further inhibition. Thus, the dual accessibility cannot be

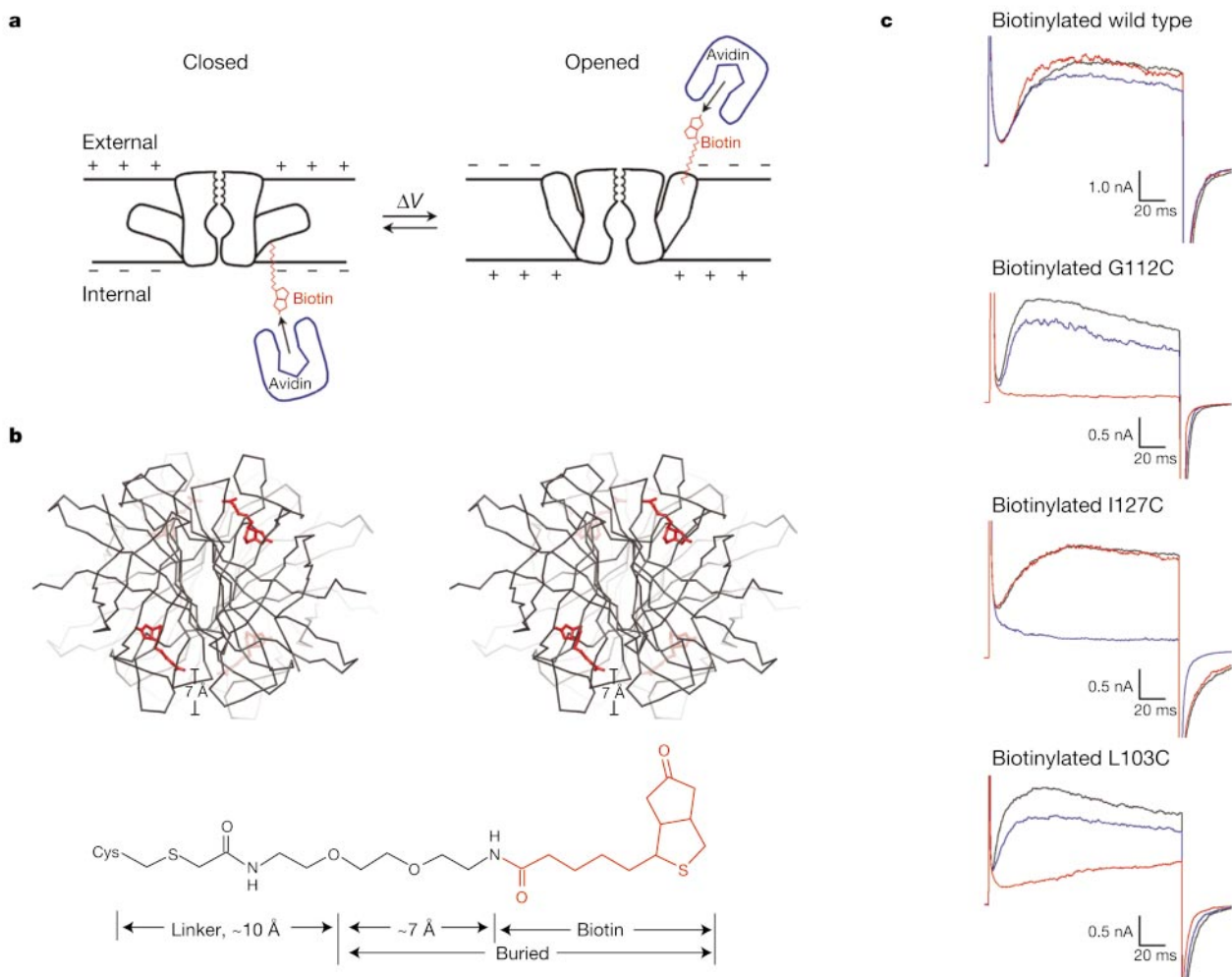


**Figure 2** Using avidin and tethered biotin as a molecular ruler to measure positions of the voltage-sensor paddles. **a**, Experimental strategy: KvAP channels with biotin tethered to a site-directed cysteine can be 'grabbed' by avidin in solution to affect channel function. **b**, Stereo view of an avidin tetramer ( $\alpha$  trace, Protein Data Bank code 1AVD) with biotin (red) in its binding pockets. Chemical structure of biotin and its PEO-iodoacetyl linker with

buried (inside avidin) and exposed segments indicated. **c**, Representative traces showing the effects of avidin on wild-type and mutant biotinylated KvAP channels. Currents were elicited with depolarizing steps in the absence (black traces) or presence of internal (blue traces) or external (red traces) avidin.

ascribed to two structurally distinct populations of channels. We conclude that positions 121 and 122 actually drag biotin and its linker all the way across the lipid membrane from the solution on one side to that on the other when the channel gates. This finding is very important, because it indicates that the voltage-sensor paddles must move a large distance through the membrane, and that they must move through a lipid environment where a bulky chemical structure such as biotin and its linker (Fig. 2b) would be unimpeded. Biotin and its linker could not be dragged through the core of a protein, as would be required by conventional models, which invoke an S4 helix buried within the protein.

### Discussion

Positional constraints on the voltage-sensor paddles are summarized in Fig. 5a, b. Horizontal solid lines show the external and internal surfaces of the cell membrane (~35 Å thick) and dashed lines show the 10 Å limit from the membrane surface set by the linker length (Fig. 2b). If the α-carbon of a cysteine residue comes within 10 Å of the membrane surface, then avidin can bind to the attached biotin, otherwise the biotin is inaccessible. Avidin is too

large to enter crevices on the channel, so it cannot penetrate below the membrane surface.

At negative membrane voltages when the channel is closed, no positions are accessible to the external side; all residues on the voltage-sensor paddles in their channel-closed position must lie deeper in the membrane than the 10-Å limit below the external surface (Fig. 5a). At negative voltages, the blue and yellow residues on S4 bind from inside, and therefore must come within 10 Å of the internal solution. The red residues, including all of S3b, the tip of the paddle and the first helical turn into S4, are protected from both sides at negative voltages and must therefore lie further than 10 Å from both surfaces; that is, between the two dashed lines. This pattern of accessibility in the closed (negative voltage) conformation constrains the voltage-sensor paddles to lie near the internal surface of the membrane with S3b above S4, as shown (Fig. 5a), similar to the orientation in the crystal structure<sup>4</sup>.

At positive membrane voltage when the channel is opened, the entire S3b helix, the tip of the paddle and the first two-and-a-half helical turns of S4 become accessible to external avidin and must therefore be within 10 Å of the external solution (Fig. 5b). The next

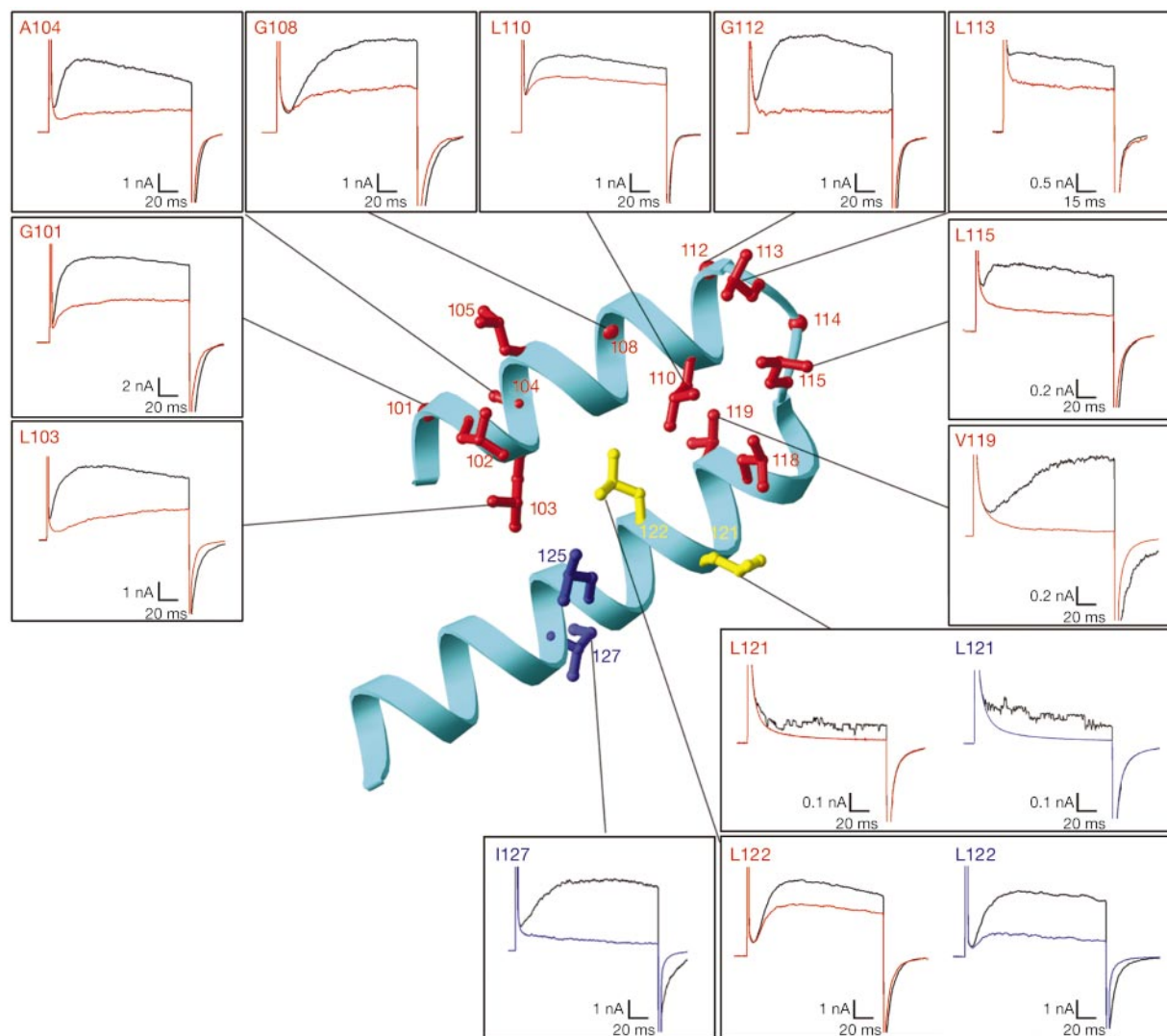


**Figure 3** Accessibility of voltage-sensor paddle residues to the internal and external sides of the membrane. Membrane was depolarized every 120 s in the absence (control) or presence of avidin on the internal and external side of each biotinylated mutant. Red side chains on the voltage-sensor paddle and selected traces indicate inhibition by avidin from the external side only; blue side chains and selected traces indicate inhibition by avidin

from the internal side only; yellow side chains and blue and red traces indicate inhibition by avidin from both sides. Black traces show control currents before avidin addition and coloured traces show currents after adding avidin. Each trace is the average of 5–10 measured traces, with the exception of the single traces for position 121.

helical turn on S4 (positions 125 and 127, blue residues) remains more distant than 10 Å from the external surface. The Fabs inform us that, in the opened conformation, two helical turns of S3b and one turn of S4 must actually protrude clear into the external solution, otherwise the epitope would not be exposed (Fig. 1b). The Fabs and pattern of avidin accessibility in the opened (positive voltage) conformation constrain the voltage-sensor paddles to be near the external membrane surface with a more vertical orientation, as shown (Fig. 5b).

In moving from their closed to their opened position, the voltage-sensor paddles' centre of mass translates approximately 20 Å (assuming a membrane thickness of 35 Å) through the membrane from inside to out, and the paddles tilt from a somewhat horizontal to a more vertical orientation. Arginines 117, 120, 123 and 126, the first four arginines on S4 (Fig. 1a), are distributed along the paddles. In the closed conformation, arginines 126, 123 and perhaps 120 can probably extend their positively charged guanidinium group to the internal lipid head group layer, whereas arginine 117 is near the internal side but still within the membrane. In the opened conformation, arginines 117, 120 and probably 123 can extend to the external solution or lipid head group layer, whereas 126 is near the external side but still within the membrane. The near-complete transfer of these four arginine residues across the membrane (in each of the four subunits) is compatible with the total gating charge in the *Shaker* K<sup>+</sup> channel of 12–14 electrons (3.0–3.5 electrons per subunit)<sup>15–17</sup>, and with the demonstration that each of these four arginine residues carries approximately one electron charge unit<sup>16,17</sup>.

A positional aspect of the voltage-sensor paddles not constrained by these experiments is whether they lie tangential to the channel's outer surface or whether they point in a radial direction away from it. The flexible S3 loops and S4–S5 linkers probably do not constrain the paddles much. However, we have two reasons for thinking that the paddles are positioned tangentially, which is the way they are positioned in Fig. 5c. First, the paddles are oriented tangentially in the crystal structure of the full channel; and second, the crystal structure of the isolated voltage sensor shows interesting salt-bridge interactions between S4 and S2, and between S3a and S2 (ref. 4). A tangential orientation would favour salt-bridge interactions between arginine residues on the voltage-sensor paddles and acidic residues on the S2 and S3a helices. Studies by Papazian and co-workers on the *Shaker* K<sup>+</sup> channel indeed suggest that salt-bridge pairs are important, and that they might exchange as the paddles

move between their closed and opened positions on the outer perimeter of the channel<sup>18–20</sup>.

To a first approximation, we describe the voltage-sensor paddles as hydrophobic cations that carry gating charges through the lipid bilayer. Ionic interactions between S4 arginines and S2 and S3 acidic residues probably assist the gating charge movement, and the presence of a polar, sometimes acidic loop between S3b and S4 in certain voltage-dependent K<sup>+</sup> channels (for example, the *Shaker* K<sup>+</sup> channel<sup>21</sup>) raises interesting questions about the structure of the lipid–water interface above the paddles when they are in their closed channel position. However, there is no escaping the basic finding that the paddles are located at the protein–lipid interface, and move while contacting the lipid membrane. Given that the paddles move through a lipid environment, it is interesting to ask why the basic residues on the voltage-sensor paddles are nearly always arginine and not lysine? One reason is that arginine (pK<sub>a</sub> ≈ 12.5 in water) will nearly always move through the membrane with a protonated, charged side chain, whereas lysine (pK<sub>a</sub> ≈ 10.5 in water) will sometimes be unprotonated. Another reason may be that arginine can easily participate in multiple hydrogen bonds (perhaps with acidic side chains) in a spatially directed way. Yet a third possible reason is that it might be energetically less costly to transfer from water to lipid the diffuse positive charge on a guanidinium group (arginine) than the more focused charge on an amino group (lysine). Studies of the transfer of hydrophobic peptides from water to octanol by White and co-workers<sup>22</sup> provide evidence for this idea by showing that the charged lysine side chain is energetically more costly in this assay than the charged arginine by about 1.0 kcal mol<sup>-1</sup>. Given that four voltage-sensor paddles must move through the membrane to open the pore, we might expect there to be a strong evolutionary bias in favour of arginine over lysine. In this regard, it is interesting that the recent structure of MscS, a mechanosensitive channel, has two basic amino acids in its transmembrane segments that are arginine<sup>23</sup>. MscS is not gated by voltage *per se*, but its mechanical force-induced opening can be modulated by voltage<sup>24</sup>, and the candidate residues that are proposed to underlie voltage modulation are arginine, not lysine<sup>23</sup>.

On the basis of the KvAP crystal structure<sup>4</sup>, the deduced positions of its voltage-sensor paddles in the functioning channel (Fig. 5a, b), and previous studies of opened and closed K<sup>+</sup> channels<sup>25,26</sup>, we propose a model for how membrane voltage gates the pore (Fig. 5c, d). This is a working model to envision how the electromechanical coupling process might occur, and it will need to be revised as more data are obtained. In the closed conformation (Fig. 5c), the positively charged voltage-sensor paddles (red) are near the intracellular membrane surface, held there by the large electric field (mean value >10<sup>7</sup> V m<sup>-1</sup>) imposed by the negative resting membrane voltage. In this conformation, the S5 and S6 (outer and inner) helices are arranged as they are in KcsA, a closed K<sup>+</sup> channel<sup>25</sup>; favourable packing interactions between the inner helices have been proposed to help to stabilize the closed conformation<sup>27</sup>. In response to depolarization, the voltage-sensor paddles move across the membrane to their external position, which exerts a force on the S4–S5 linker, pulling the S5 helices away from the pore axis (Fig. 5d). The crystal structure of KvAP shows that the S5 helices form a cuff outside the S6 helices, and suggests that when the S5 cuff is expanded, the S6 helices follow, opening the pore<sup>4</sup>.

Although previous mutational studies of voltage-dependent gating have been interpreted in the context of the conventional models, many of the data are consistent with the structural model presented here, and indeed help to constrain it. For example, second-site suppressor mutations in the *Shaker* K<sup>+</sup> channel suggest that certain salt bridges probably break and reform as the voltage-sensor paddles move<sup>20</sup>. In addition to four S4 arginine residues, a component of the gating charge in *Shaker* was shown to come from an S2 acidic residue (glutamate 293, corresponding to aspartate 72 in KvAP)<sup>16</sup>, implying that S2 might change its position in the membrane as the

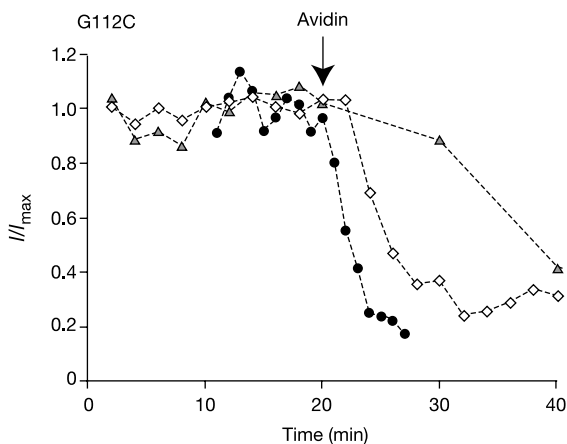


**Figure 4** Exposure of the voltage-sensor paddle to the external solution occurs only when the membrane is depolarized. For the biotinylated G112C mutant, normalized (to the average control) currents elicited by depolarization to 100 mV every 60 s (circles), 120 s (diamonds) and 600 s (triangles) are shown before and after the addition of avidin to the external side.

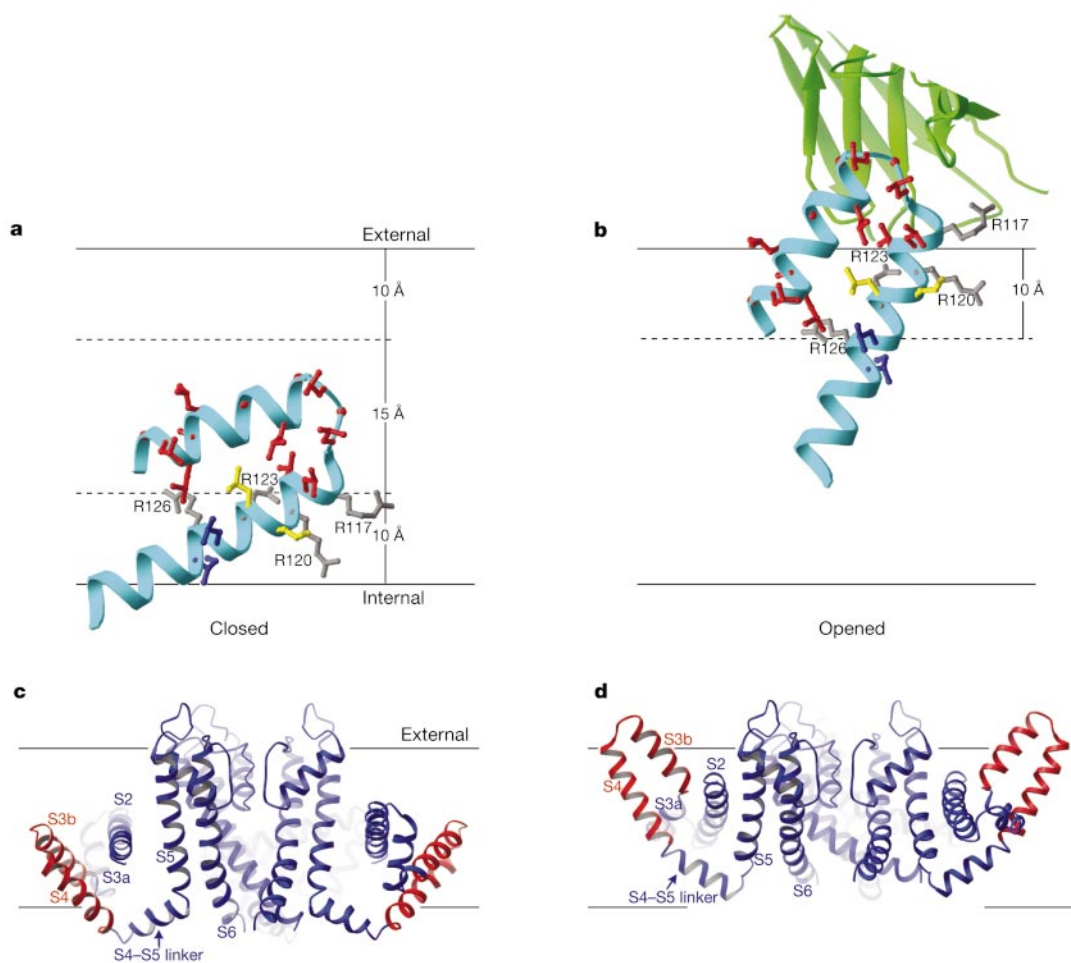


**Figure 5** Positions within the membrane of the voltage-sensor paddles during closed and opened conformations, and a hypothesis for coupling to pore opening. **a, b**, Closed (**a**) and opened (**b**) positions of the paddles derived from the tethered biotin–avidin measurements, and structural and functional measurements with Fabs. A voltage-sensor paddle is shown as a cyan ribbon with side chains colour-coded as in Fig. 3. Grey side chains show four arginine residues on the paddle, and the green ribbon (**b**) shows part of a

bound Fab from the crystal structures. Solid horizontal lines show the external and internal membrane surfaces, and dashed lines indicate the 10-Å distance from the surfaces set by biotin and its linker. **c**, The closed KvAP structure is based on the paddle depth and orientation in **a** (red), and adjusting the S5 and S6 helices of KvAP to the positions in KcsA, a closed K<sup>+</sup> channel. **d**, The opened KvAP structure is based on the paddle depth and orientation in **b** (red), and the pore of KvAP.

voltage-sensor paddles move; the loose attachment of S2 to the pore in the KvAP crystal structure certainly would allow this to happen. Disulphide cross-linking of S4 to the turret loop between S5 and the pore helix<sup>28</sup>, and of two S4 segments within a tetramer to each other<sup>29</sup> (an observation that was very difficult to understand in the context of conventional models), are in agreement with the mobile voltage-sensor paddles in Fig. 5c, d. The accessibility of thiol-reactive compounds to cysteine residues introduced into the *Shaker* K<sup>+</sup> channel S4 (refs 30–32), and the ability of histidine residues to shuttle protons across the membrane<sup>33</sup>, are in reasonable agreement with our data on voltage-sensor paddle movements. However, our structural and mechanistic interpretation, summarized in Fig. 5, differs fundamentally from past models of voltage-dependent gating. This new picture is based on the elucidation of the voltage-sensor paddle structure, its flexible attachments and disposition relative to the pore, and the paddles' positions in the membrane when the channel is closed and opened.

## Conclusion

Here and in an accompanying paper<sup>4</sup>, we have shown that (1) the gating charges are carried on voltage-sensor paddles, which are helix–turn–helix structures attached to the channel through flexible

S3 loops and S4–S5 linkers; (2) the paddles are located at the channel's outer perimeter and move within the lipid membrane; (3) the S2 helices lie beside the pore and contain acidic amino acids that could help to stabilize positive charges on the paddles as they move across the membrane; (4) the total displacement of the voltage-sensor paddles is approximately 20 Å perpendicular to the membrane; and (5) the large displacement of the paddles could open the pore by pulling on the S4–S5 linker. We conclude that the voltage sensor operates by an extraordinarily simple principle based on hydrophobic cations attached to levers, which enables the membrane electric field to perform mechanical work to open and close the ion-conduction pore. □

## Methods

### Biotinylation

All biotinylation studies were carried out using a KvAP channel in which the single endogenous cysteine was mutated to serine (C247S). This mutant showed no detectable electrophysiological differences when compared to wild-type KvAP. Single cysteine mutations were then added to the voltage-sensor paddle (positions 101 to 127) using the QuickChange method (Stratagene) and confirmed by sequencing the entire gene. Mutant channels were expressed and purified by the same protocol as wild-type KvAP channels<sup>5</sup>, except that before gel filtration, mutant KvAP channels were incubated with 10 mM DTT for 1 h. Immediately after gel filtration, mutant channels (at 0.5–1.0 mg ml<sup>-1</sup>) were

incubated with 500  $\mu\text{M}$  PEO-iodoacetylbiotin (Pierce) for 2–3 h at room temperature, and then either reconstituted into lipid vesicles for electrophysiological analysis, or purified away from the excess biotin reagent on a desalting column, complexed with avidin (Pierce) and run on an SDS gel to assess the extent of biotinylation.

**Electrophysiology**

Fabs (6E1 and 33H1) and VSTX1 were purified as described in the companion paper<sup>4</sup> and used in electrophysiological assays. Electrophysiological studies of wild-type and biotinylated KvAP channels were carried out as described<sup>5</sup>. To measure inhibition, Fabs (~500 nM), VSTX1 (30 nM) or avidin (40  $\mu\text{g ml}^{-1}$ ) were added to wild-type and/or cysteine-mutant, biotinylated channels reconstituted into lipid membranes, and studied using various voltage protocols.

Received 19 February; accepted 11 March 2003; doi:10.1038/nature01581.

1. Sigworth, F. J. Voltage gating of ion channels. *Q. Rev. Biophys.* **27**, 1–40 (1994).
2. Armstrong, C. M. & Bezanilla, F. Charge movement associated with the opening and closing of the activation gates of the Na<sup>+</sup> channels. *J. Gen. Physiol.* **63**, 533–552 (1974).
3. Bezanilla, F. The voltage sensor in voltage-dependent ion channels. *Physiol. Rev.* **80**, 555–592 (2000).
4. Jiang, Y. *et al.* X-ray structure of a voltage-dependent K<sup>+</sup> channel. *Nature* **423**, 33–41 (2003).
5. Ruta, V., Jiang, Y., Lee, A., Chen, J. & MacKinnon, R. Functional analysis of an archaeobacterial voltage-dependent K<sup>+</sup> channel. *Nature* **422**, 180–185; advance online publication, 2 March 2003 (doi:10.1038/nature01473).
6. Swartz, K. J. & MacKinnon, R. Mapping the receptor site for hanatoxin, a gating modifier of voltage-dependent K<sup>+</sup> channels. *Neuron* **18**, 675–682 (1997).
7. Slatin, S. L., Qiu, X. Q., Jakes, K. S. & Finkelstein, A. Identification of a translocated protein segment in a voltage-dependent channel. *Nature* **371**, 158–161 (1994).
8. Qiu, X. Q., Jakes, K. S., Finkelstein, A. & Slatin, S. L. Site-specific biotinylation of colicin Ia. A probe for protein conformation in the membrane. *J. Biol. Chem.* **269**, 7483–7488 (1994).
9. Qiu, X. Q., Jakes, K. S., Kienker, P. K., Finkelstein, A. & Slatin, S. L. Major transmembrane movement associated with colicin Ia channel gating. *J. Gen. Physiol.* **107**, 313–328 (1996).
10. Pugliese, L., Coda, A., Malcovati, M. & Bolognesi, M. Three-dimensional structure of the tetragonal crystal form of egg-white avidin in its functional complex with biotin at 2.7 Å resolution. *J. Mol. Biol.* **231**, 698–710 (1993).
11. Zagotta, W. N., Hoshi, T., Dittman, J. & Aldrich, R. W. Shaker potassium channel gating. II. Transitions in the activation pathway. *J. Gen. Physiol.* **103**, 279–319 (1994).
12. Zagotta, W. N., Hoshi, T. & Aldrich, R. W. Shaker potassium channel gating. III. Evaluation of kinetic models for activation. *J. Gen. Physiol.* **103**, 321–362 (1994).
13. Schoppa, N. E. & Sigworth, F. J. Activation of Shaker potassium channels. III. An activation gating model for wild-type and V2 mutant channels. *J. Gen. Physiol.* **111**, 313–342 (1998).
14. Cole, K. S. & Moore, J. W. Potassium ion current in the squid giant axon: dynamic characteristic. *Biophys. J.* **1**, 1–14 (1960).
15. Schoppa, N. E., McCormack, K., Tanouye, M. A. & Sigworth, F. J. The size of gating charge in wild-type and mutant Shaker potassium channels. *Science* **255**, 1712–1715 (1992).
16. Seoh, S. A., Sigg, D., Papazian, D. M. & Bezanilla, F. Voltage-sensing residues in the S2 and S4 segments of the Shaker K<sup>+</sup> channel. *Neuron* **16**, 1159–1167 (1996).
17. Aggarwal, S. K. & MacKinnon, R. Contribution of the S4 segment to gating charge in the Shaker K<sup>+</sup> channel. *Neuron* **16**, 1169–1177 (1996).

18. Papazian, D. M. *et al.* Electrostatic interactions of S4 voltage sensor in Shaker K<sup>+</sup> channel. *Neuron* **14**, 1293–1301 (1995).
19. Tiwari-Woodruff, S. K., Lin, M. A., Schulteis, C. T. & Papazian, D. M. Voltage-dependent structural interactions in the Shaker K<sup>+</sup> channel. *J. Gen. Physiol.* **115**, 123–138 (2000).
20. Papazian, D. M., Silverman, W. R., Lin, M. C., Tiwari-Woodruff, S. K. & Tang, C. Y. Structural organization of the voltage sensor in voltage-dependent potassium channels. *Novartis Found. Symp.* **245**, 178–190 (2002).
21. Gonzalez, C., Rosenman, E., Bezanilla, F., Alvarez, O. & Latorre, R. Periodic perturbations in Shaker K<sup>+</sup> channel gating kinetics by deletions in the S3–S4 linker. *Proc. Natl Acad. Sci. USA* **98**, 9617–9623 (2001).
22. Wimley, W. C., Creamer, T. P. & White, S. H. Solvation energies of amino acid side chains and backbone in a family of host-guest pentapeptides. *Biochemistry* **35**, 5109–5124 (1996).
23. Bass, R. B., Strop, P., Barclay, M. & Rees, D. C. Crystal structure of *Escherichia coli* MscS, a voltage-modulated and mechanosensitive channel. *Science* **298**, 1582–1587 (2002).
24. Martinac, B., Buechner, M., Delcour, A. H., Adler, J. & Kung, C. Pressure-sensitive ion channel in *Escherichia coli*. *Proc. Natl Acad. Sci. USA* **84**, 2297–2301 (1987).
25. Doyle, D. A. *et al.* The structure of the potassium channel: molecular basis of K<sup>+</sup> conduction and selectivity. *Science* **280**, 69–77 (1998).
26. Jiang, Y. *et al.* The open pore conformation of potassium channels. *Nature* **417**, 523–526 (2002).
27. Yifrach, O. & MacKinnon, R. Energetics of pore opening in a voltage-gated K<sup>+</sup> channel. *Cell* **111**, 231–239 (2002).
28. Laine, M. *et al.* Structural interactions between voltage sensor and pore in the Shaker K<sup>+</sup> channels. *Biophys. J.* **82**, 231a (2002).
29. Aziz, Q. H., Partridge, C. J., Munsey, T. S. & Sivaprasadarao, A. Depolarization induces intersubunit cross-linking in a S4 cysteine mutant of the Shaker potassium channel. *J. Biol. Chem.* **277**, 42719–42725 (2002).
30. Larsson, H. P., Baker, O. S., Dhillon, D. S. & Isacoff, E. Y. Transmembrane movement of the Shaker K<sup>+</sup> channel S4. *Neuron* **16**, 387–397 (1996).
31. Yusuf, S. P., Wray, D. & Sivaprasadarao, A. Measurement of the movement of the S4 segment during the activation of a voltage-gated potassium channel. *Pflügers Arch.* **433**, 91–97 (1996).
32. Baker, O. S., Larsson, H. P., Mannuzzu, L. M. & Isacoff, E. Y. Three transmembrane conformations and sequence-dependent displacement of the S4 domain in Shaker K<sup>+</sup> channel gating. *Neuron* **20**, 1283–1294 (1998).
33. Starace, D. M., Stefani, E. & Bezanilla, F. Voltage-dependent proton transport by the voltage sensor of the Shaker K<sup>+</sup> channel. *Neuron* **19**, 1319–1327 (1997).

**Acknowledgements** We thank D. Gadsby and O. Andersen for helpful discussions and advice on the manuscript. This work was supported in part by a grant from the National Institutes of Health (NIH) to R.M. V.R. is supported by a National Science Foundation Graduate Student Research Fellowship, and R.M. is an Investigator in the Howard Hughes Medical Institute.

**Competing interests statement** The authors declare that they have no competing financial interests.

**Correspondence** and requests for materials should be addressed to R.M. (mackinn@rockvax.rockefeller.edu).